

Spatial Evolution of Velocity-Modulated Ion Beams in a Plasma

Noriyoshi Sato, Hideo Sugai, and Rikizo Hatakeyama

Department of Electronic Engineering, Tohoku University, Sendai, Japan

(Received 29 October 1974)

Spatial growth and damping of a velocity-modulated ion beam are observed in a Q machine where no ion-ion instability is predicted. The phenomena are well explained by linear "wave" theory for beam bunching.

The behavior of modulated ion beams in a plasma is of current interest in conjunction with plasma instability and heating. Several experiments on ion-ion instability have reported that perturbations grow spatially as a result of the instability, but saturate and damp subsequently.¹ Here we present another feature of perturbations produced in an ion-beam-plasma system, clearly demonstrated in a double-plasma (DP)-type Q machine. Similar spatial growth and damping appear under some conditions even if the system is stable. Linear "wave" theory for beam bunching² explains the phenomena well.

Two collisionless 4-cm-diam Na plasmas are produced in a Q machine³ which is operated as a DP machine,⁴ as shown in Fig. 1(a). One of them, the "driver plasma," is surrounded by a small metal cylinder tied to the hot plate HP_D . The hot plate HP_T of the other plasma, the "target plasma," is grounded, together with the vacuum chamber. Electrons of the two plasmas are separated from each other by a negatively biased grid G_s . With a positive bias ϕ_B of HP_D with respect to HP_T , ions of the driver plasma flow into the target plasma [$N_p = (0.2-5.0) \times 10^8 \text{ cm}^{-3}$, $T_e \approx T_i \approx 0.2 \text{ eV}$] as an ion beam. The beam current is almost independent of ϕ_B ($\geq 0.2 \text{ V}$). The beam energy is estimated by an energy analyzer to be a little (10% or so) smaller than $e\phi_B$. Its density N_b , $10^6-10^8 \text{ cm}^{-3}$, is controlled by the density of the driver plasma. Assuming a half-Maxwellian velocity distribution for ions emitted from HP_D , we estimate the beam temperature T_b ,⁶ which decreases with an increase in ϕ_B . The condition $T_b \ll T_i \approx T_e$ is easily realized. Numerical analysis does not predict ion-ion instability under this condition. The beam velocity is modulated by superposing small voltage variations ϕ on ϕ_B . Spatial evolutions of the perturbations are measured by a movable grid G_R biased negatively.

Typical interferometer outputs⁵ for sinusoidal modulation are shown in Fig. 1(b). For small

values of $\epsilon (=N_b/N_p)$, the perturbations grow spatially, but saturate and damp subsequently, as in the case of ion-ion instability. As ϵ increases, however, there appears a periodic change of growth, saturation, and damping. Its pitch l decreases with an increase in ϵ . Figure 2 shows the dependence of the phenomena on ϕ_B . For $\phi_B \leq 1.2 \text{ V}$, almost exponential damping is observed. The wavelength λ , the damping distance δ , and δ/λ increase as ϕ_B increases. The phase velocities are larger than the beam speed V_b in this range of ϕ_B . The periodic growth and damping are observed for $\phi_B \geq 3 \text{ V}$ and then the phase velocities around the amplitude maxima are nearly equal to V_b . The periodic change of amplitude suggests that the wave patterns consist of two waves. Their phase velocities can be calculated from λ and l [see Fig. 2(b)]. The same results are also obtained by the ordinary grid excitation⁵ using G_E or G_s in Fig. 1(a).

Figure 3 shows a typical measurement of the spatial evolution for ramp modulation. A pulse-shaped perturbation is observed to grow along the beam up to the distance x_0 where the amplitude begins to saturate. Beyond there, only the width spreads gradually. With an increase of ϕ_B and/or τ (rise time of the ramp voltage), x_0 becomes large.

For $e\phi_B \gg \kappa T_i$, under which the periodic change of amplitude appears, we can neglect ion response to the modulated ion beam in the target plasma. If there is no collective interaction, ballistic bunching² may be applied to the phenomena. Suppose that an ion beam is velocity-modulated sinusoidally at $x=0$, i.e., $v_b(x=0, t) = v_0 \cos(\omega t)$. Then the ω component of the perturbed ion-beam current $j_b(x, t)$ is predicted to be $N_b V_b J_1(\omega x/V_b) \times (v_0/V_b) \sin[\omega(x/V_b - t)]$, because $e\phi_B \gg \kappa T_b$ and $j_b(x=0, t) = 0$ in the experiment. Thus, the envelope is expressed by the first-order Bessel function whose argument depends on v_0 ($\propto \phi$), in contrast to our observations.

In the presence of collective interaction, the

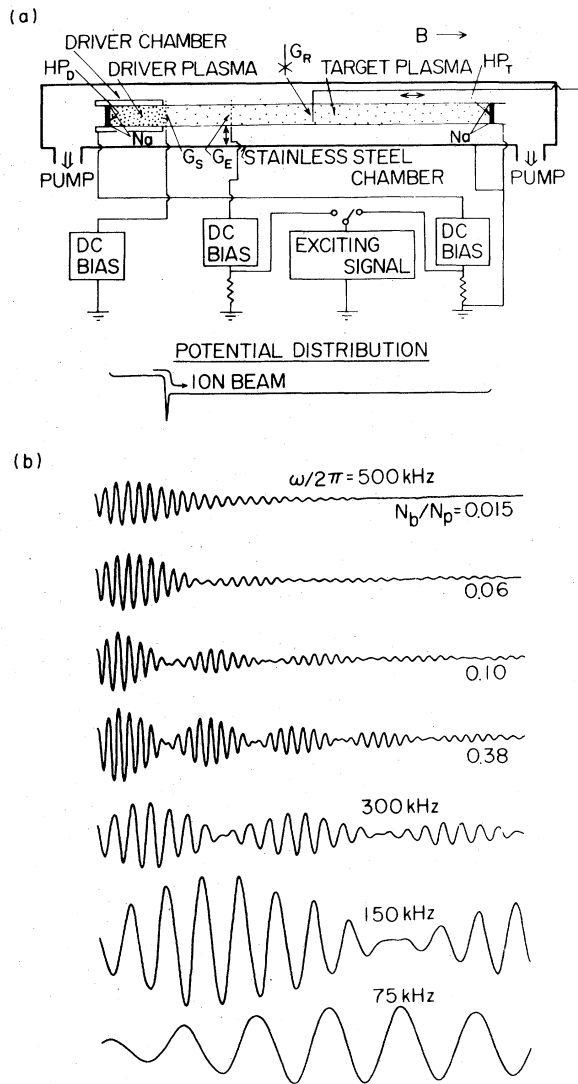


FIG. 1. (a) Schematic of experimental setup. A screen grid G_s is made of 0.03-mm-diam wires spaced 0.5 mm apart. A grid G_e , made of 0.2-mm-diam wires spaced 2 mm apart, is used only for ordinary grid excitation (Ref. 5). (b) Typical wave patterns for sinusoidal modulation with frequency $\omega/2\pi$, demonstrating their dependence on N_b/N_p and $\omega/2\pi$ at $\phi_B = 8$ V. The starting point is 3 cm from G_s . Full scan is 63.2 cm. Detector-sensitivity calibration gives almost the same results for various values of ω if the normalized distance $\omega x/V_b$ (V_b is the beam speed) is adopted. The wave patterns do not depend on ϕ in the range 0.005–0.1 V peak to peak except that the amplitudes are proportional to ϕ . For larger values of ϕ , we cannot neglect signals reflected from HP_T .

beam bunching is illustrated as an interference of fast and slow beam modes.² We can assume the Boltzmann relation for electrons, charge neutrality, and $T_b = 0$. Thus, the necessary equa-

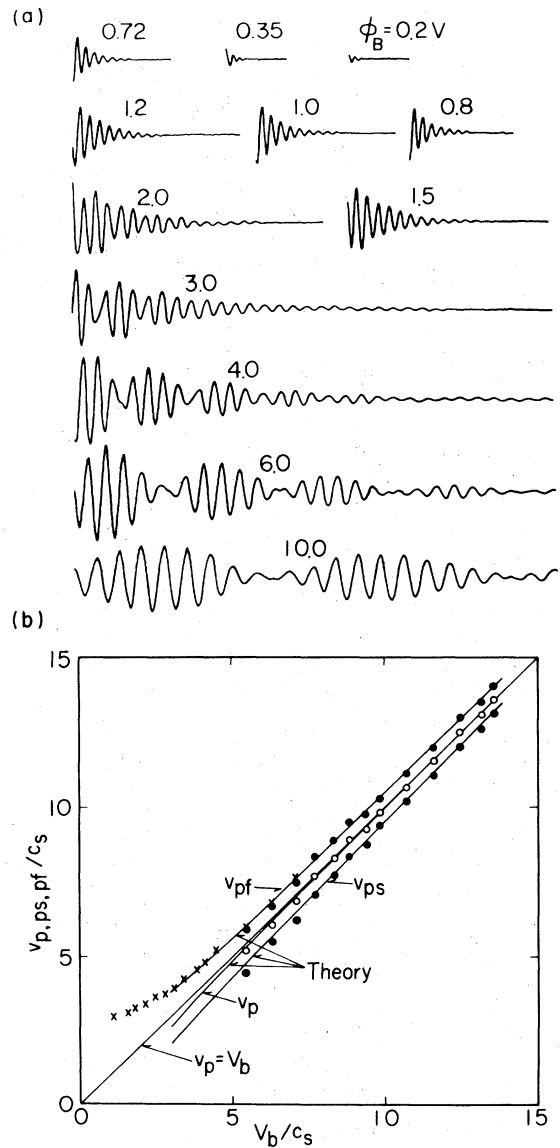


FIG. 2. (a) Dependence of wave pattern on ϕ_B . (b) Phase velocities as a function of ion-beam speed V_b [$C_s = (\kappa T_e/M)^{1/2}$]. Crosses show phase velocities for small values of ϕ_B at which the damping is exponential. For large values of ϕ_B , periodic growth and damping are observed. Open circles show phase velocities around the amplitude maxima. The periodic change of amplitude is attributed to interference of two waves whose phase velocities are given by closed circles. Theoretical values are shown by solid lines.

tions are

$$\frac{\partial n_b}{\partial t} + V_b \frac{\partial n_b}{\partial x} + N_b \frac{\partial v_b}{\partial x} = 0, \tag{1}$$

$$\frac{\partial v_b}{\partial t} + V_b \frac{\partial v_b}{\partial x} + \frac{C_s^2}{N_p} \frac{\partial n_b}{\partial x} = 0, \tag{2}$$

where $C_s^2 = \kappa T_e / M$, and $n_b(x, t)$ and $v_b(x, t)$ are perturbed ion-beam density and velocity, respectively. Introducing the Fourier transform in time and the Laplace transform in space,

$$A(x, t) = \int_{-\infty}^{+\infty} A(x, \Omega) \exp(-i\Omega t) d\Omega / 2\pi, \quad A(k, \Omega) = \int_0^\infty A(x, \Omega) \exp(-ikx) dx,$$

we obtain, after simple algebra,

$$\frac{j_b(k, \Omega)}{N_b V_b} = i \frac{v_b(x=0, \Omega) \Omega}{V_b^2} \frac{V_b^2 - \epsilon C_s^2}{(\Omega - kV_b)^2 - k^2 \epsilon C_s^2}. \tag{3}$$

For sinusoidal modulation, $v_b(x=0, \Omega) = \pi v_0 [\delta(\Omega + \omega) + \delta(\Omega - \omega)]$ [$\delta(\xi)$ is the delta function]. The inverse transformations of $j_b(k, \Omega)$ yield

$$\frac{j_b(x, t)}{J_b} = \frac{v_0}{V_b} \frac{v_{pf} v_{ps}}{V_b \epsilon^{1/2} C_s} \sin\left(\omega x \frac{\epsilon^{1/2} C_s}{v_{pf} v_{ps}}\right) \sin\left[\omega \left(\frac{V_b}{v_{pf} v_{ps}} x - t\right)\right], \tag{4}$$

where $J_b = N_b V_b$, and v_{pf} ($= V_b + \epsilon^{1/2} C_s$) and v_{ps} ($= V_b - \epsilon^{1/2} C_s$) are phase velocities of fast and slow ion-beam modes, respectively. The phase velocity of this interference pattern, v_p , is equal to $v_{pf} v_{ps} / V_b$. The shape of the envelope is independent of φ .

Ramp modulation yields $v_0(x=0, \Omega) = v_0 \{\pi \delta(\Omega) + [\exp(i\Omega\tau) - 1] / \Omega^2 \tau\}$. Then we get

$$\frac{j_b(x, t)}{J_b} = \frac{v_0}{V_b} \frac{v_{pf} v_{ps}}{2V_b \epsilon^{1/2} C_s \tau} \left(-\frac{x - v_{pf}(t - \tau)}{v_{pf}} \theta(x - v_{pf}(t - \tau)) + \frac{x - v_{pf}t}{v_{pf}} \theta(x - v_{pf}t) \right. \\ \left. + \frac{x - v_{ps}(t - \tau)}{v_{ps}} \theta(x - v_{ps}(t - \tau)) - \frac{x - v_{ps}t}{v_{ps}} \theta(x - v_{ps}t) \right), \tag{5}$$

where $\theta(\xi)$ is the step function. This equation yields a pulse-shaped perturbation which develops as shown ($a_b/V_b = 0$) in Fig. 3. The growth of $j_b(x, t)$ is given by $v_p x / V_b^2 \tau$ up to the distance $x_0 = [v_{pf} v_{ps} \tau / (v_{pf} - v_{ps})]$ where the amplitude saturates. Beyond there, only the pulse width spreads gradually.

The above theory provides an essential mechanism of the phenomena. In order to explain other characteristics, however, we must extend the analysis to $T_b \neq 0$. Assume a shifted Maxwellian velocity distribution for the ion beam. Then, for $V_b \gg a_i$ [$= (2\kappa T_i / M)^{1/2}$] and $\epsilon^{1/2} C_s \gg a_b$ [$= (2\kappa T_b / M)^{1/2}$], v_{pf} and v_{ps} are given by $v_{pf, s} \approx V_b \pm \epsilon^{1/2} C_s \times (1 + 3T_b / T_e)^{1/2}$ which are plotted, together with $v_p (= v_{pf} v_{ps} / V_b)$, in Fig. 2(b). A good agreement between experiment and theory is found in this figure. The other effect of T_b is the wave damping. For $V_b \gg a_i$ and $\epsilon^{1/2} C_s \gg a_b$, with an increase of V_b and/or ϵ , the damping factors of fast and slow modes, β_f and β_s , decrease in such a manner that $\beta_s - \beta_f$ (> 0) becomes small. This is the reason why clear interference patterns are observed for large values of V_b and ϵ . For small values of V_b and/or ϵ , the slow mode damps more strongly than the fast mode, and so its contribution to the wave patterns is negligible especially far away from G_s . Moreover, for $e\phi_B \leq T_e$, the slow mode cannot propagate in the direction of the beam velocity. Thus, it is well

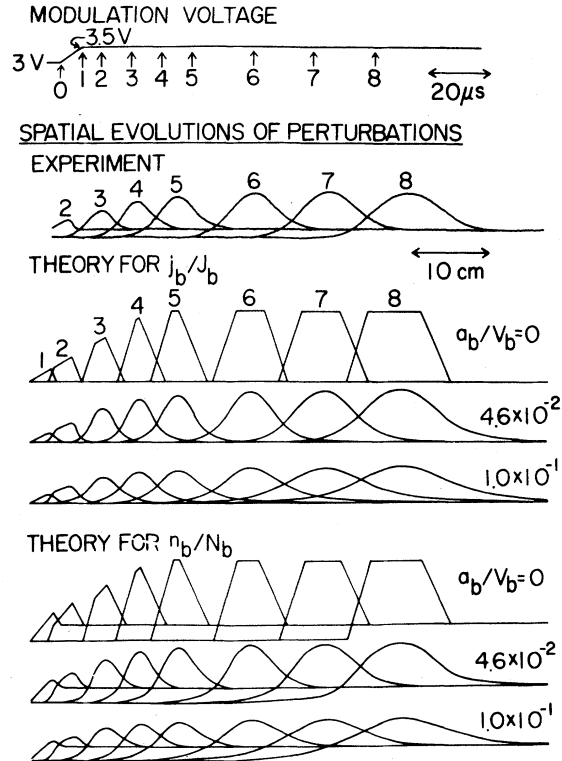


FIG. 3. Measured and predicted spatial evolutions for ramp modulation. The starting point is $x = 3$ cm for experiment and $x = 0$ cm for theory.

understood that the measured phase velocities coincide with v_{pf} for $\varphi_B \approx 1.2$ V at which the damping is observed to be exponential.

Predicted evolutions of ramp-modulated perturbations for $a_b/V_b \neq 0$ are shown in Fig. 3, where both $j_b(x,t)/J_b$ and $n_b(x,t)/N_b$ are included. In the experiment, G_R is biased negatively to pick up ion currents. The estimated value⁶ of a_b/V_b is 0.046 for $\varphi_B = 3$ V. A good agreement between measured and predicted evolutions is found in Fig. 3.

The simplest way to prove our explanation is to make an experiment on pulse modulation. In fact, there appear positive and negative pulses which are easily confirmed to correspond to fast and slow ion-beam modes.

In our work, ions of the target plasma play no significant role. Thus, the situation is equivalent to a single-ended Q machine under an "electron-rich" condition, in which an ion beam flows through electrons.⁷ An important difference is that V_b can be arbitrarily controlled in the DP-type Q machine. In this work, collective interaction plays an important role for low-frequency perturbations produced in a Q machine, in contrast to the analyses emphasizing the nonexistence of such an interaction in an ideal Q machine.⁸ The phenomena observed should always exist in an ion-beam-plasma system. In ion-beam shocks,⁹ the same phenomena can be found before the shock formation. Only slow modes were picked up in recent work on nonlinear ion-beam modes using DP machines¹⁰; but our work shows that both fast and slow ion-beam modes of nearly equal amplitude propagate along the beam.

We thank Professor Y. Hatta for his encouragement. Discussions with Professor H. Ikezi and

Dr. K. Saeki were fruitful.

¹D. R. Baker, *Phys. Fluids* **16**, 1730 (1973); R. J. Taylor and F. V. Coroniti, *Phys. Rev. Lett.* **29**, 34 (1972); Y. Kiwamoto, *J. Phys. Soc. Jpn.* **37**, 466 (1974). See also related theories and experiments referred to in the above papers.

²Much work was done on electron-beam bunching in conjunction with klystrons. When a collective (space-charge) effect is significant, the bunching is ascribed to propagations of fast and slow beam modes produced via velocity modulation [see, for example, W. W. Harman, *Fundamentals of Electronic Motion* (McGraw-Hill, New York, 1953), p. 204].

³N. Rynn and N. D'Angelo, *Rev. Sci. Instrum.* **31**, 1326 (1960).

⁴R. J. Taylor, K. R. MacKenzie, and H. Ikezi, *Rev. Sci. Instrum.* **43**, 1675 (1972).

⁵N. Sato, H. Sugai, A. Sasaki, and R. Hatakeyama, *Phys. Rev. Lett.* **30**, 685 (1973).

⁶ T_b is defined by $N_b \kappa T_b = M \int_{-\infty}^{\infty} (v - V_b)^2 f_b(v) dv$. In the presence of φ_B , a truncated Maxwellian distribution is assumed for $f_b(v)$. Then

$$T_b/T = 1 + 2\pi^{-1/2} \alpha \exp(-\alpha^2)(1 - \operatorname{erf} \alpha)^{-1} - 2\pi^{-1} \exp(-2\alpha^2)(1 - \operatorname{erf} \alpha)^{-2},$$

where $\alpha = (e\varphi_B/\kappa T)^{1/2}$ (T is the temperature of HPD). For $\alpha \gg 1$, $T_b/T \approx (1 - 3/2\alpha^2)/2\alpha^2$.

⁷J. M. Buzzi, H. J. Doucet, and D. Gresillon, *Phys. Fluids* **13**, 3041 (1970).

⁸J. L. Hirshfield and J. H. Jacob, *Phys. Fluids* **11**, 411 (1968); K. Estabrook and I. Alexeff, *Phys. Rev. Lett.* **29**, 573 (1972).

⁹H. Ikezi, T. Kamimura, M. Kako, and K. E. Lonngren, *Phys. Fluids* **16**, 2167 (1973).

¹⁰R. A. Stern, J. F. Decker, and P. M. Platzman, *Phys. Rev. Lett.* **32**, 359 (1974); A. Lee, S. Gleman, and W. D. Jones, *Phys. Rev. Lett.* **32**, 1225 (1974). It is only Kiwamoto who observed two beam modes in a DP machine (see Ref. 1).

Filamentation and Subsequent Decay of Laser Light in Plasmas*

A. Bruce Langdon and Barbara F. Lasinski

University of California, Lawrence Livermore Laboratory, Livermore, California 94550

(Received 11 April 1974)

It has been predicted that an intense light beam in a plasma will break up into a number of self-focused filaments. We show that as a result of filamentation, strong plasma heating can occur in a wider range of densities than has been expected. The laser light decays into lower frequency modes which then heat the electrons and assist in the further development of a narrow filament.

Plasma heating by intense electromagnetic waves is an essential aspect of laser fusion schemes. The heating mechanisms mostly con-

sidered occur near the critical density surface, where the local electron plasma frequency ω_{pe} equals the laser frequency ω_0 . Mechanisms